processes

MDPI

Article

An Experimental Study of Wall Effect on a Hot Settling Sphere in a Newtonian-Fluid-Contained Block Using Photography

Mojtaba Ashouri [1], Mohammad Hasan Kayhani [2,*] and Mohsen Nazari [2]

[1] Kharazmi International Campus, Shahrood University of Technology, Shahrood P.O. Box 3619995161, Iran
[2] Faculty of Mechanical and Mechatronics Engineering, Shahrood University of Technology, Shahrood P.O. Box 3619995161, Iran
* Correspondence: h_kayhani@shahroodut.ac.ir; Tel.: +98-9121732330

Abstract: In this study, the effect of temperature on the velocity and trajectory of a hot sphere falling in a water block was experimentally investigated. The sphere, 12 mm in diameter, was thrown through the water inside an enclosure at the ambient temperature by an electromagnetic attachment mechanism, and the particle velocity was recorded by a high-speed camera at 2000 fps. Then, using an image-processing algorithm, the real-time particle location was extracted and its velocity was measured. The results of the cold sphere falling test were compared with those obtained from the numerical solving by the governing equations. An electric heater was used to heat the sphere up to 100, 200, and 300 °C in order to investigate the effect of temperature on the sphere. The sphere was thrown upon reaching the desired temperature. By increasing the temperature, the sphere's velocity was increased up to around 40% of the velocity of the cold sphere. Further, the sphere was thrown from a point in the vicinity of the wall to investigate the wall impact on the particle movement. This led the sphere to deviate from its trajectory, with the deviation in the cold sphere being negligible, i.e., around 30% of the sphere's diameter. However, the rate of deviation was much more notable upon increasing the temperature. The deviation start point varied depending on the sphere's temperature, with the highest deviation that was observed for a sphere with a temperature of 100 °C. Ultimately, the sphere traveled in a more extended way, with no deviation from the main trajectory, when its temperature was increased.

Keywords: sphere fall; image processing; heat transfer

Citation: Ashouri, M.; Kayhani, M.H.; Nazari, M. An Experimental Study of Wall Effect on a Hot Settling Sphere in a Newtonian-Fluid-Contained Block Using Photography. *Processes* **2023**, *11*, 248. https://doi.org/10.3390/pr11010248

Academic Editors: Gholamreza Kefayati, Hasan Sajjadi and Udo Fritsching

Received: 6 December 2022
Revised: 30 December 2022
Accepted: 4 January 2023
Published: 12 January 2023

1. Introduction

Particle motion in fluids is a high-potential field of study for various natural, industrial, and biological processes, including chemical processes and power particles, sea engineering, environment engineering and deep-sea mining [1], drug delivery, etc. As a classic problem, particle motion has been investigated within various numerical and experimental studies [2]. Reducing the particle resistance which occurs while particles move through fluids is a major issue which has been addressed by previous studies. Reduced resistance leads to higher sphere velocity and lower energy dissipation [3]. A wide range of parameters affects the motion of a particle falling into a fluid, including particle shape, density, surface roughness, fluid type, and the temperature difference between the particle and the fluid. Mehrabian et al. [4] studied the separation of a settling surface-coated sphere in an oil as a function of the adhesion ratio and surface tension. Mehri et al. [5] experimentally investigated the effect of grooves on a settling sphere's surface upon entering a Newtonian fluid and the sphere's motion in the fluid. They estimated the particle's trajectory, velocity, and acceleration based on the number of grooves.

Terminal velocity and solid particle trajectory through a fluid are the most important issues addressed by previous scholars. A settling particle in a fluid maintains its accelerated motion until the sum of gravity and resistance forces, such as buoyancy and the drag force

(dependent on the drag coefficient), becomes zero. In this case, the particle velocity is called the terminal or settling velocity [6]. The drag coefficient is one of the most important hydrodynamic forces acting on a settling sphere. It is caused by friction and the pressure gradient between the fluid and the sphere [7]. Many researchers have focused on the numerical investigation of a settling cold sphere. Jalaal et al. [6] used the homotopy method (HPM) to solve the equations governing a settling sphere and to calculate the time-dependent particle velocity. Nouri et al. [8] used several analytical methods to evaluate the time-dependent behavior of settling spherical particles in water. The DTM, DTM-Padé approximation, Galerkin (GM), and numerical methods have been proposed for assessing the fall of three aluminum, copper, and lead spheres. The results indicated that the DTM-Padé approximation was adequately accurate and convergent. Yang et al. [9] compared the drag coefficient and terminal velocity equations obtained by the numerical solution of the governing equations. Rooki et al. [10] proposed a new method for predicting the settling velocity of spherical particles in Newtonian and non-Newtonian fluids. They also compared their results with a broad range of previous numerical and experimental studies. Although a significant number of numerical methods have been used by previous studies to solve the governing equations, the experimental studies are few. Hazzab et al. [11] provided one of the first experimental methods to achieve the settling velocity of particles. They used a stopwatch to experimentally measure the average velocity of the settling particle in a fluid with different viscosity and showed that the sphere's velocity is highly dependent on the shape and diameter of the particle and, more importantly, on the Reynolds number of the solid particle. They proposed a model for direct calculation by using the dependence of the velocity of non-spherical particles with the sphere of the same. The model is successfully validated for isometric particles. Another way to experimentally measure the velocity is to use an optical sensor for detecting the particle passing different locations in the fluid. Kheloufi et al. [12] employed this method to determine the effect of viscosity on settling sphere tracking. They estimated the fluid viscosity by photographing the motion of a settling sphere inside a thin tube and using an optical spectrum. However, the recent development in high-speed cameras has contributed to the precise evaluation of the unsteady motion of particles inside a fluid. The simultaneous falling of two spheres has also been widely addressed in numerical and experimental studies. For example, Sulaymon et al. [13] evaluated the falling of two steel spheres in a side-by-side and back-to-back motion in a non-Newtonian fluid and assessed the effect of the initial distance on the spheres' behavior. Dash et al. [14] conducted a similar experimental and numerical study and provided sphere size, trajectory, velocity, and hydrodynamic forces in a dimensionless manner as a function of the Reynolds number. Another field of study regarding particles settling in a fluid is the effect of walls on particle motion. Most studies have focused on the case where the particle was far enough from the walls. However, some scholars have addressed the particle velocity and trajectory affected by the walls and compared the results with that of the away-from-the-wall case. Luo et al. [15] numerically studied a sphere's trajectory falling near the wall and observed a rotational behavior. They found irregular rotations and zigzag movement by the particle near the wall, which could be caused by the wall and vortex effects. Tsai et al. [16] studied the motion of spherical and non-spherical particles near the wall and showed the irregular and unconventional motion of the particles near the wall. Near-the-wall motion can be considered for simulating intravascular motions. Fidleris et al. [17] experimentally simulated the particle motion within a cylindrical vessel and studied the effect of near-the-wall motion.

As discussed before, different methods have been proposed for reducing the particle resistance inside the fluid, some of which are based on changing the sphere. Some methods usually change the physical properties of the sphere's surface (e.g., roughness, elasticity, etc.), and some focus on fluid density. Previous studies have addressed the surface temperature (or the temperature difference between the particle surface and fluid) and heat transfer during the particle's fall [3]. Due to the complicity of temperature variation and convection heat transfer around a falling particle, most previous studies have concentrated on simpli-

fied problems (e.g., 2D and single particle) with low Reynolds and Grashof numbers using numerical methods [18]. Strom et al. [19] used the multiphase DNS numerical method to study the solid particle motion considering thermal effects. Hashemi et al. [20] addressed the falling of a spherical particle with thermal effects using a 3D Boltzmann network. Their results demonstrated that the density and temperature ratios were the most important parameters for the trajectory and behavior of the particle's motion. Majlesara et al. [21] numerically studied hot and cold settling spheres and evaluated the effect of different parameters on the drag coefficient. Gylys et al. [3] studied a hot settling sphere in a water-filled container, evaluating the sphere size, material, and Leidenfrost effect. They showed a direct correlation between the velocity and surface temperature of the sphere. As the surface temperature increases, the velocity increases by up to 30%. Similar research was conducted by [22,23] on a hot settling sphere with a particular temperature and its effect on the sphere's velocity and location. Their results confirmed the Leidenfrost effect on increasing sphere velocity and reducing drag coefficient. The sphere's entry into the water from a certain distance, the formation of a moving cavity, and the experimental evaluation of the sphere's trajectory and velocity using photography (relative to the motion time) were carried out by Mehri et al. [24] for a single hot, grooved sphere and by Wang et al. [25] to evaluate the interactive effect of two spheres settling side-by-side and the formed cavities.

The literature includes a wide range of numerical studies. Few experimental studies have been conducted, most of which focused on the velocity of a cold settling sphere away from the wall. However, in many applications, including industries or biotechnology applications, variable temperature and distance from the wall became important. Therefore, as it appears necessary to investigate, the current study addresses cold and hot settling spheres in water as a Newtonian fluid. The wall effect on the hot and cold sphere velocity and trajectory is also discussed.

2. Laboratory Setup

The schematic laboratory setup is shown in Figure 1. A 15 × 15 × 75 fully transparent glass container filled with water at the ambient temperature was used to assess the settling sphere. The water temperature was constantly monitored by a sensor to prevent any water temperature fluctuations and their potential effects on the test. A holding mechanism held the sphere near the water surface (<5 mm from the surface). The designed holding mechanism was accurately installed above the water surface (Figure 1) and included a 24 V and 1.5 A inductive electromagnet controlled by a switch cutting off the magnet. The electromagnet was made of steel alloy M530 to avoid residual magnetism and ensure the immediate release of the sphere. The sphere was made of stainless steel with a diameter of 12 mm.

The test is conducted to evaluate the falling of the hot sphere in a water-contained block. An electrical heater is employed to heat up the sphere to evaluate the effect of the sphere's temperature on its velocity and trajectory. The sphere is initially heated up to a temperature above the target temperature and is installed on the electromagnetic holding mechanism by a special pair of tongs. An infrared thermometer constantly monitors the sphere's temperature (KIRAY 300). When the sphere reaches the target temperature, the electromagnet is instantly cut off and the sphere is released. The velocity and trajectory of the settling sphere were evaluated at four temperatures: ambient, 100, 200, and 300 °C. Two different release cases were considered for the test. First, the sphere was released exactly in the center of the container; therefore, the wall effects were neglected. For the second case, the sphere was released at a 0.5 d from the wall to assess the wall effects on the sphere's motion.

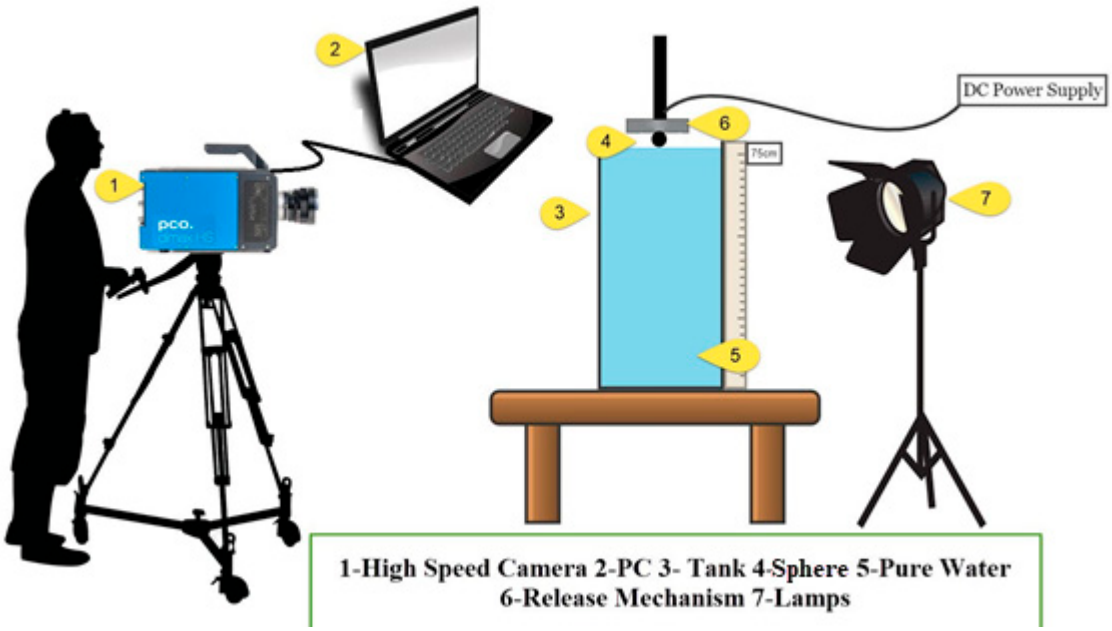

(**a**)

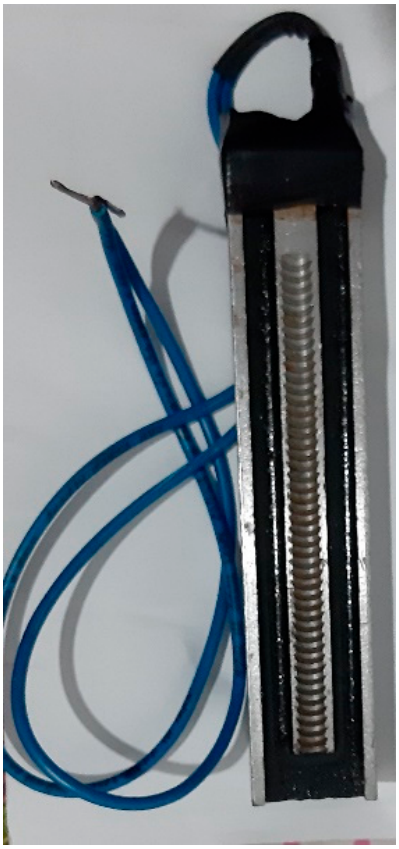

(**b**)

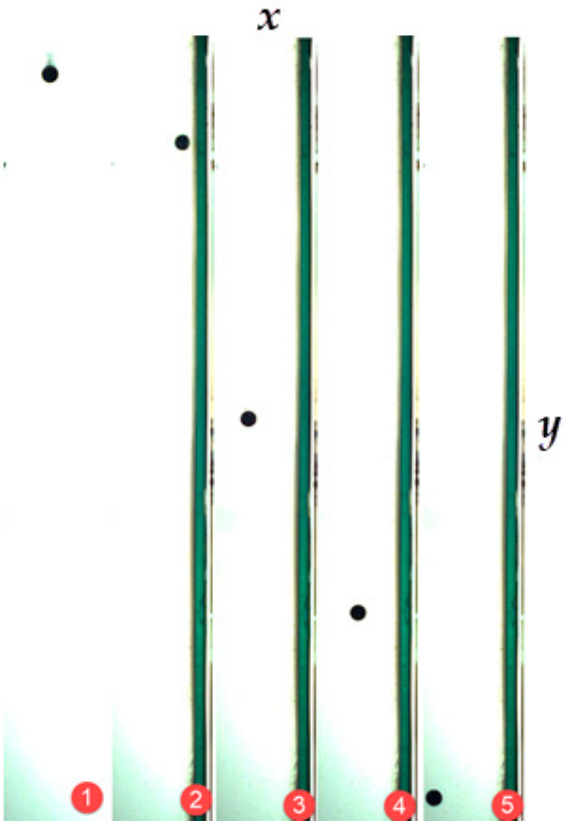

(**c**)

Figure 1. (**a**) The schematic laboratory setup, (**b**) magnetic holder, and (**c**) one of the captured images at different non-dimensional times: (1) the sphere at 300 °C away from the wall for t* = 0.08, (2) the sphere at the ambient temperature near the wall at t* = 19 (where t* is non dimensional time), (3) the sphere at 100 °C near the wall at t* = 47, (4) the sphere at 200 °C near the wall at t* = 72, and (5) the sphere at 300 °C near the wall at t* = 0.94.

2.1. Image Processing

The main objective of the tests conducted by the current study is to determine the sphere's location and, consequently, its trajectory and velocity. To this end, a high-speed camera was used to photograph the sphere's location at any moment; then, the images were processed using the algorithm implemented to determine the velocity and acceleration of the sphere. The images were made by the high-speed 5400 fps PCO Dimax camera (85 mm Carl-Zeiss lens and a focal length of 1.4) with a maximum resolution of 1008 × 1008 pixels. For our study, the images were taken at the speed of 2000 fps. The camera was installed at the height of 110 cm and the distance of 150 cm from the container, and could take 550 mm long images. Two wide-beam lamps were used for background lighting to reduce image noise.

2.2. Error Analysis

We tried our best to minimize errors while measuring and recording the results. However, each test was repeated three times and the results were used based on the 95% confidence interval to improve the accuracy and reliability of the recorded data. The uncertainty of the parameters was calculated using the Backwith method [26] (Equation (1)).

$$\begin{aligned} \sigma &= \sqrt{\frac{\sum (x_i - \bar{x})}{n-1}} \\ \sigma_v &= \frac{\sigma}{\sqrt{n}} \\ \frac{U_v}{v} &= \sqrt{\sum \left(\frac{U_p}{p}\right)^2} \end{aligned} \tag{1}$$

where U_v is variable uncertainty and U_p is related to parameter uncertainties. The instrument error and the calculated uncertainty of different parameters are listed in Table 1.

Table 1. Instrument error and error analysis.

Parameter	Instrument Error	Uncertainty Error
Length	±1.0 mm	-
Temperature	±5 °C	-
Velocity	-	1.5%
Reynolds number	-	2.2%
Drag coefficient	-	2.1%

3. Results and Data Analysis

3.1. Cold Settling Sphere (Away from the Wall)

A cold settling sphere in water is the most fundamental case. Numerical equations can be used to determine the velocity and drag coefficient of the settling sphere at the ambient temperature, and the results can be compared to the derived experimental data.

As Buckingham π theorem suggests, and considering the parameters involved in the problem solving, the dimensionless parameters, including the Reynolds number and the drag coefficient, can be calculated by Equations (2) and (3).

$$Re = \frac{\rho u D}{\mu} \tag{2}$$

$$C_D = \frac{1}{2}\frac{F}{\rho u^2 A} \tag{3}$$

where Re is Reynolds Number [-], C_D is drag coefficient [-], p is density [kg/m^3], u is velocity [m/s], D is sphere diameter [m], μ is viscosity of a fluid [kg/ms], F is force [N], and A is area [m^2]. The Basset equation for the unsteady motion of a particle inside a fluid

is presented in Equation (4) regarding the falling of a particle with a higher density than the fluid and neglecting the Basset history force.

$$m_s \frac{du}{dt} = mg\left(1 - \frac{\rho}{\rho_s}\right) - \frac{C_D}{8}\pi D^2 \rho u^2 - \frac{1}{12}\pi D^3 \rho \frac{du}{dt} \quad (4)$$

where m_s is sphere mass [kg], g is gravity [m/s^2], and t is time [s]. Equation (4) represents the buoyancy, drag, and additional gravity force caused by the acceleration of the flow around the particle. The equation is complicated due to the nonlinear nature of the drag coefficient. For a broad range of Reynolds numbers (<105), Ferreira [27] proposed an approximate equation for drag coefficient using experimental data (Equation (5)). Jalaal et al. [6] showed that Equation (5) is the most accurate expression for estimating the drag coefficient.

$$C_D = \frac{24}{Re}\left(1 + \frac{Re}{48}\right) \quad (5)$$

Finally, Equation (4) can be rewritten as

$$\frac{1}{12}\pi D^3(2\rho_s + \rho)\frac{du}{dt} + 3\pi D\mu ut + \frac{1}{16}\pi D^2 \rho u^2 - \frac{1}{6}\pi D^3 g(\rho_s + \rho) = 0;\ u(0) = 0 \quad (6)$$

The coefficients are determined based on the physical conditions, fluid properties, and sphere size. Equation (6) is a nonlinear equation with initial boundary conditions that can be solved analytically or numerically. For our study, Equation (6) was solved by the Runge–Kutta–Fehlberg method with the order of error of 5 (RKF45) as a function of time to compare the solution with the experimental results, since we were focused on the experimental method.

The photographs were taken after releasing the sphere, and were saved within a certain time interval (i.e., 0.001 s). The designed algorithm derived the particle's location in each image and calculated the instantaneous velocity of the sphere according to the sphere's displacement relative to the previous image. The sphere settles into water under the influence of gravity, buoyancy, and drag forces. The falling velocity of the sphere was high due to the gravity force and the insignificant resisting forces. As the sphere falls through the water, the resisting forces eventually equal the driving force. The tests reveal that the sphere's velocity became constant after a short while, which is called the terminal velocity. The numerical results also confirm the same. Figure 2a compares the dimensionless sphere velocity obtained by Equation (6) and the experimental velocity obtained by a 12 m sphere settling into a water container at the ambient temperature in terms of dimensionless falling time. The dimensionless velocity and time are defined by Equation (7):

$$\begin{aligned} V_{nond} &= \frac{V}{V_t} \\ t_{nond} &= \frac{t}{T} \end{aligned} \quad (7)$$

where V_t is the terminal velocity obtained by experimental results, and T is the time the sphere's velocity reaches its terminal velocity. Figure 2b shows the numerical versus the experimental result dispersion. The dispersion patterns suggest good agreement between numerical and experimental results.

The maximum difference between the experimental and numerical data was 6.5%. The difference can be attributed to the drag coefficient calculations from Equation (4) because various drag coefficient equations have been proposed by the literature. The difference can also be due to experimental imaging errors caused by lighting. Terminal sphere velocity is an important parameter. When the forces acting on the sphere are equal, i.e., the sum of buoyancy and drag forces are equal to the gravity force, the sphere is at its terminal velocity. Figure 3a compares the terminal velocities achieved by the numerical methods, experimental tests, and Gillis et al. [3]. The drag coefficient calculated by the proposed equations with a certain confidence level is presented in Figure 3b.

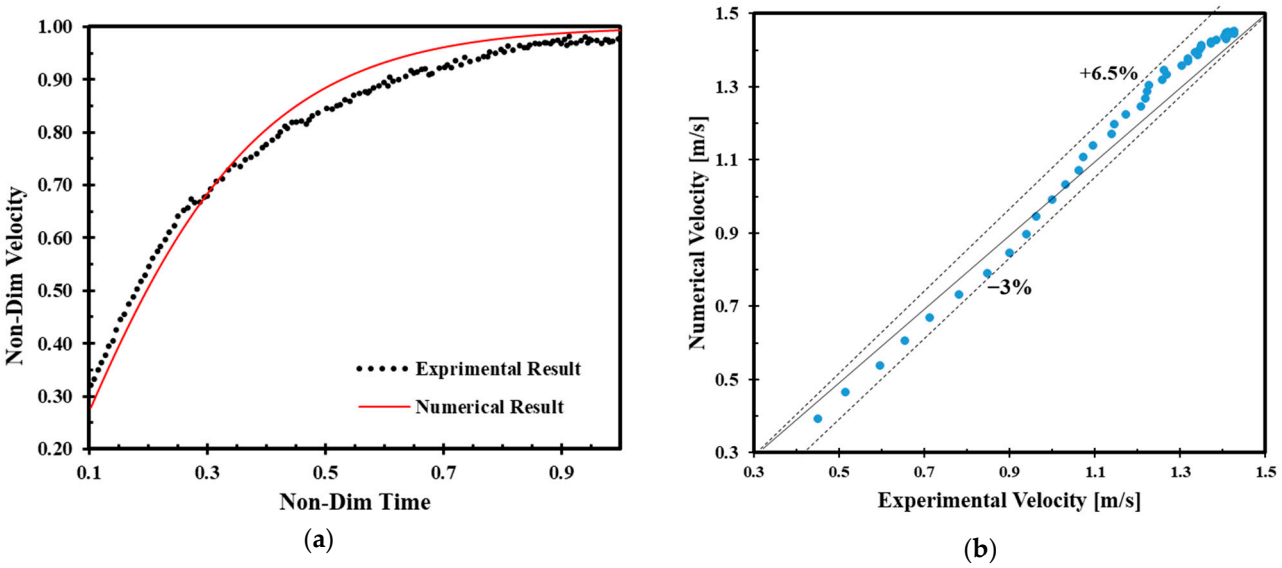

Figure 2. (**a**) Comparison of the numerical and experimental data for a cold settling sphere in the water and (**b**) comparing the result dispersion for the numerical and experimental analysis for the settling sphere (non-dimensional velocity = v/Vt where Vt is terminal velocity).

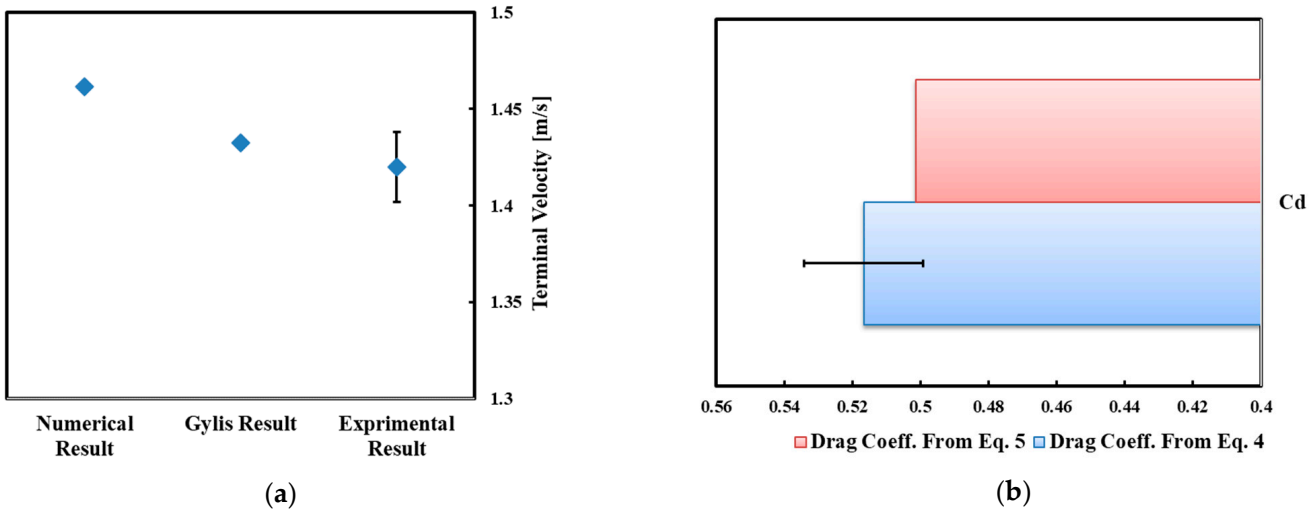

Figure 3. (**a**) The terminal velocity of the cold sphere and comparing the velocity to Gylys et al. [3] and the numerical data and (**b**) comparison of the drag coefficient obtained by the experiments and Equations (4) and (5).

3.2. Hot Settling Sphere (Away from the Wall)

As discussed before, one of the main objectives of our study was to evaluate the effect of temperature on a settling sphere's velocity and trajectory. Figure 4a,b show the trajectory versus dimensionless time and dimensionless velocity, respectively. Obviously, the sphere's velocity significantly increased for higher temperatures. A maximum increase of 40% is reported for a falling sphere in 300 °C. Figure 5 represents the instantaneous-to-terminal velocity ratio with a confidence interval error report. The sphere's velocity did not significantly change up to 100 °C. However, the velocity profoundly increased as the temperature reached 200 °C. The same trend was observed for the temperature of 300 °C. However, the velocity began to decline after reaching a certain value, and it is worth noting that the sphere returned to its terminal velocity. This might happen because the sphere's temperature would probably become the same as the fluid temperature after a while. So, the sphere would behave the same as a cold sphere. When the sphere is hot

and released into the water, a layer of vapor is formed around the sphere, increasing the sphere's velocity. Figure 6 shows the vapor film around a sphere falling with 300 °C for different non-dimensional time. As shown, a lot of micro-scale vapor bubbles are separated from the vapor film which separates the sphere from the surrounding water, in other words, the contact surface changes in a way that reduces the drag coefficient, and thus increases the velocity. Similar results were reported by Li et al. [22] for a hot settling sphere inside a fluid-containing block.

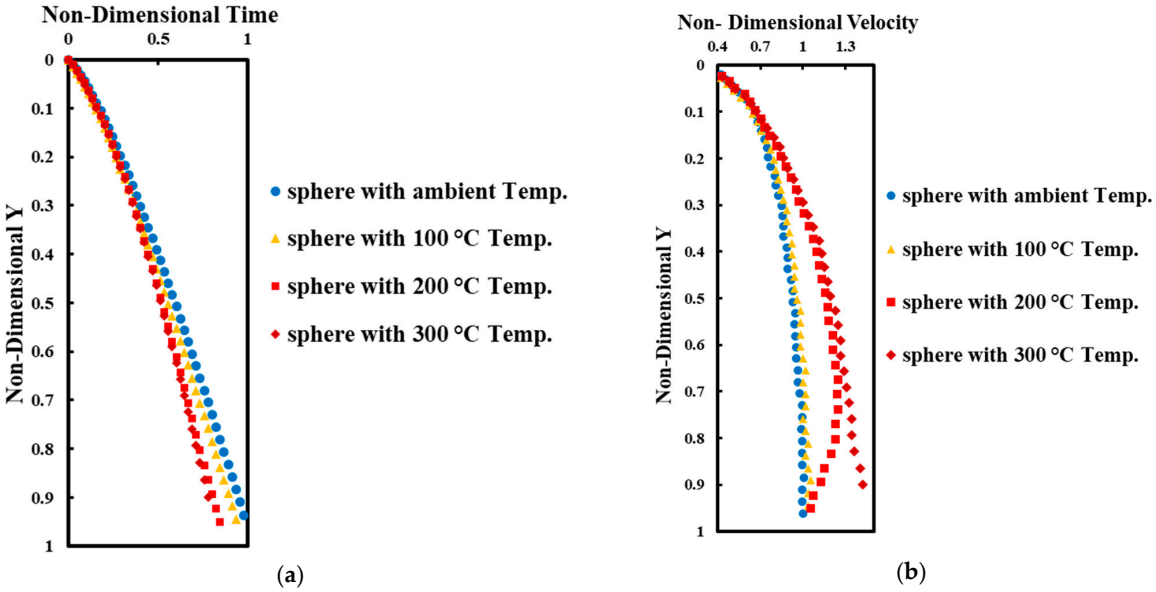

Figure 4. Vertical location of the sphere: (**a**) in terms of dimensionless time and (**b**) in terms of dimensionless velocity of the sphere at different temperatures (non-dimensional $Y = y/L$ where L is length of channel and non-dimensional time = t/T where T is the time the sphere's velocity reaches its terminal velocity).

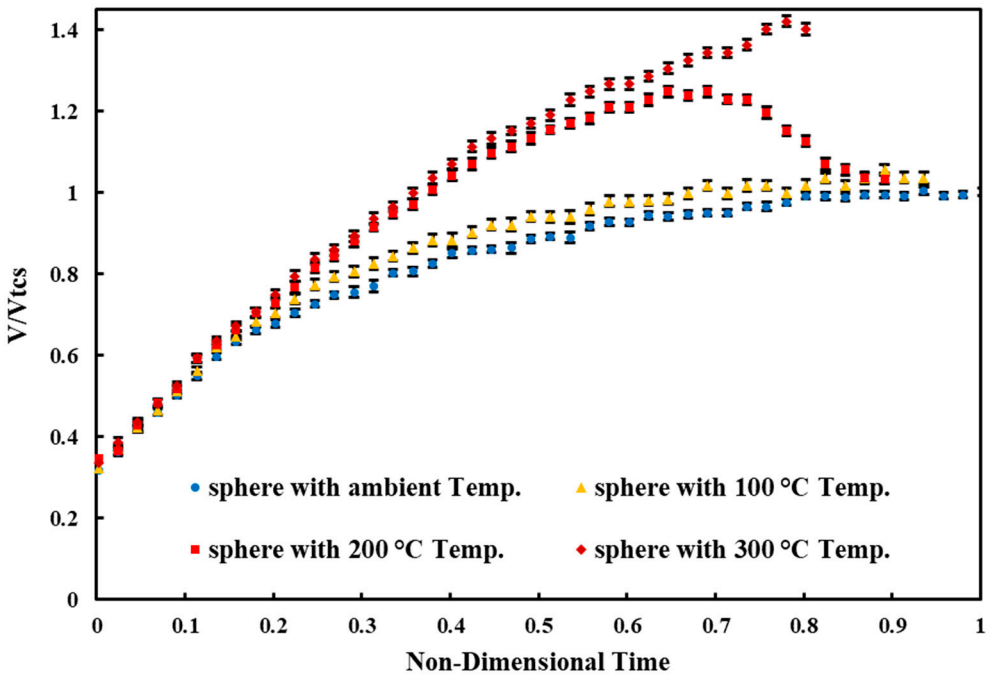

Figure 5. The dimensionless velocity versus the dimensionless time for the sphere at different temperatures where *Vtcs* is terminal velocity of cold sphere.

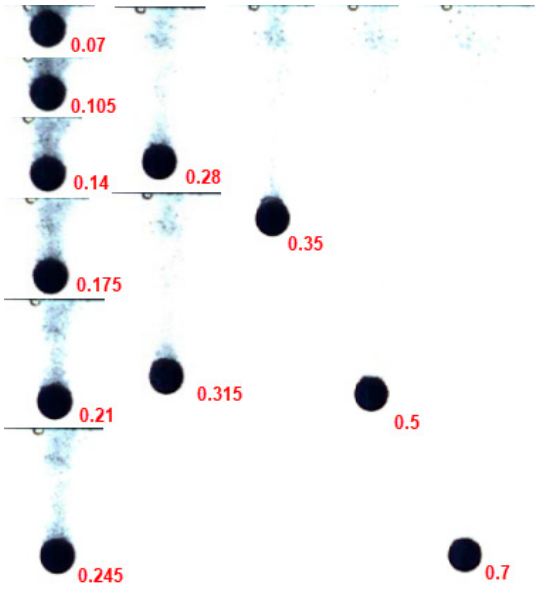

Figure 6. Vapor film around falling sphere with 300 °C at different non-dimensional time.

3.3. Releasing the Sphere near the Wall

The sphere was precisely placed near the wall (about half the diameter) and then released. Figure 7 shows the sphere's trajectory at different temperatures. As can be seen, the cold sphere slightly deviated (<5 mm) and then moved downward again. As the temperature increased, the trajectory changed significantly. When the sphere was at 100 °C, it deviated after passing about 15% of the trajectory, while hotter spheres deviated by a longer delay. As the temperature increased, the point of deviation was further down. As before, the sphere's behavior was similar at 200 and 300 °C.

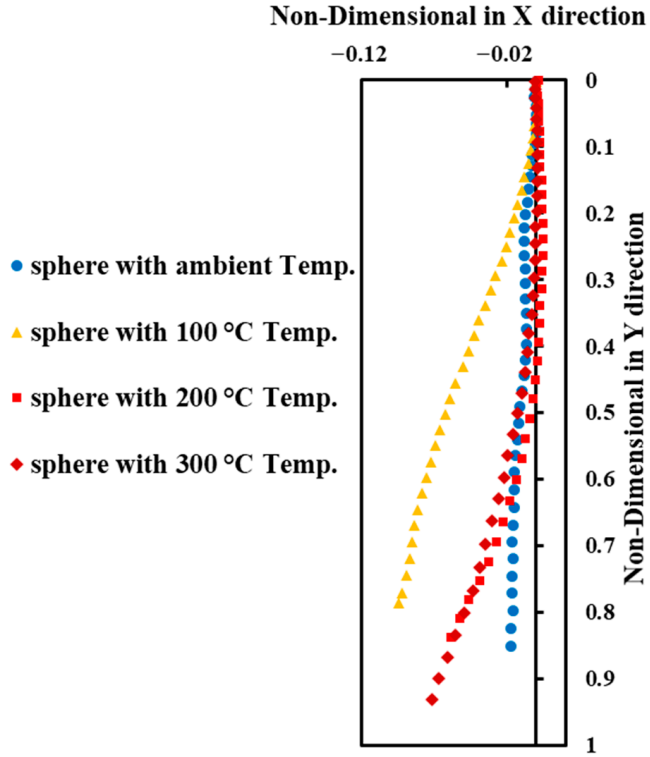

Figure 7. Settling sphere location at different temperatures near the wall.

Figure 8 shows the instantaneous velocity of the sphere at different temperatures near the wall with a confidence interval error report. Since the sphere deviates from its vertical course, Figure 9 shows the velocity along the x-axis. The results indicated that the velocity along the x-axis approached zero after a while for all cases, and the sphere's trajectory became purely vertical. The deviation led to a velocity component along the x-axis; consequently, the velocity along the y-axis was less than that of the away-from-the-wall case. However, since the velocity along the x-axis was significantly less than the velocity along the y-axis, the vertical velocity did not change significantly compared to previous cases. So, it can be concluded that the wall effect is much greater on hot spheres than on colder ones, which can be due to the interaction between the wall and the layer of vapor around the sphere.

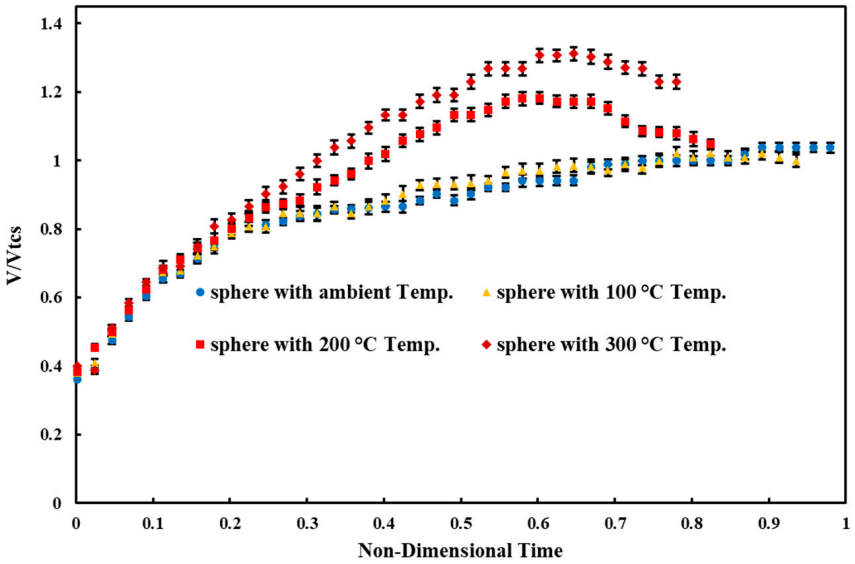

Figure 8. Dimensionless velocity versus dimensionless time for the sphere at different temperatures near the wall.

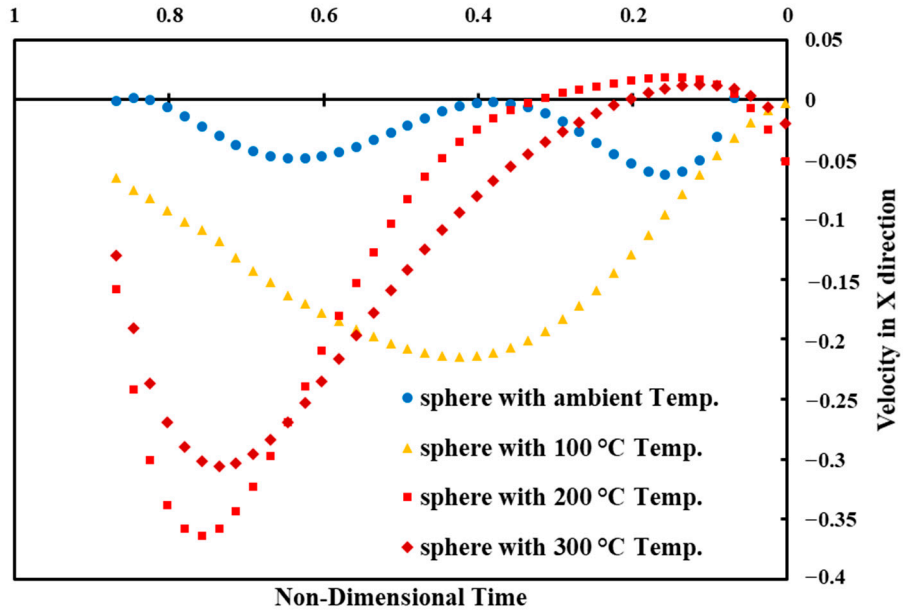

Figure 9. The horizontal velocity of the sphere versus dimensionless time for the sphere at different temperatures near the wall.

4. Conclusions

Solid particles settling into a fluid pose a frequent problem for different fields, such as environmental, marine, biotechnology, engineering, etc. This study focused on investigating the trajectory and velocity of a settling sphere in a Newtonian fluid at different temperatures. The steel sphere was 12 mm in diameter and settled into a water-contained block. The settling process was photographed with high-speed cameras. The images were analyzed using an algorithm, the location of each particle was derived, and the instantaneous velocity was calculated. The results were compared to the numerical solutions discussed. A heater was employed to heat the sphere up to a certain temperature, and the sphere was released into the water after reaching certain temperatures (100, 200, and 300 °C). First, the sphere was released far from the wall and then it was released near the wall (less than half the sphere's diameter) to evaluate the wall effect. The major findings of the study are as follows:

1. For a cold settling sphere, it was observed that after a short while, when the total force became zero, the sphere reached its terminal velocity and continued to settle at that velocity. The test results were compared to the numerical results obtained by the equations discussed in the paper, and a maximum error of 6.5% was observed, which can be caused by the proposed values for the drag coefficient.
2. Heating the sphere would change its velocity. Higher temperatures led to higher velocities. At 300 °C, the sphere's velocity increased by 40%, which can be due to the formation of a vapor layer around the sphere and the consequent drag coefficient variation. It should be noted that the velocity of the hot sphere was reduced after a while and reached the terminal velocity of the cold sphere. This can be caused by the temperature decrease after entering the water and reaching the ambient temperature. However, proper investigation of the process requires equipment capable of measuring the sphere's temperature during its trajectory. So, it can be recommended for future studies.
3. The near-the-wall settling sphere can experience deviations in the trajectory. The deviation was less than half the sphere's diameter at the ambient temperature, but the horizontal changes became significant as the temperature increased. The maximum deviation was recorded at the temperature of 100 °C, and the sphere experienced a change in its vertical trajectory after passing 15% of the trajectory. As the temperature increased, the change in the vertical trajectory was delayed. The deviation led to a horizontal velocity component, affecting the vertical one. However, since the horizontal component was insignificant, the vertical velocity was not so different from the away-from-the-wall case. The results suggested that the horizontal component was reduced after a while and ultimately became zero at the end of the fall.

Author Contributions: Conceptualization and methodology, M.A., M.N. and M.H.K.; investigation, M.A.; writing—original draft preparation, M.A.; writing—review and editing, M.N.; supervision, M.N. and M.H.K. All authors have read and agreed to the published version of the manuscript.

Funding: This research received no external funding.

Data Availability Statement: Not applicable.

Conflicts of Interest: The authors declare no conflict of interest.

References

1. Dai, Y.; Zhang, Y.; Li, X. Numerical and experimental investigations on pipeline internal solid-liquid mixed fluid for deep ocean mining. *Ocean. Eng.* **2021**, *220*, 108411. [CrossRef]
2. Zou, L.; Sun, J.Z.; Sun, Z.; Yu, Z.B.; Zhao, H.B. Study of two free-falling spheres interaction by coupled SPH–DEM method. *Eur. J. Mech.-B/Fluids* **2022**, *92*, 49–64. [CrossRef]
3. Gylys, J.; Skvorcinskiene, R.; Paukstaitis, L.; Gylys, M.; Adomavicius, A. Water temperature influence on the spherical body's falling velocity. *Int. J. Heat Mass Transf.* **2015**, *89*, 913–919. [CrossRef]
4. Mehrabian, S.; Acosta, E.; Bussmann, M. Oil–Particle Separation in a Falling Sphere Configuration: Effect of Oil Film Thickness. *Energy Fuels* **2016**, *30*, 8776–8786. [CrossRef]

5. Mehri, A.; Akbarzadeh, P. Water entry of grooved spheres: Effect of the number of grooves and impact velocity. *J. Fluids Struct.* **2021**, *100*, 103198. [CrossRef]
6. Jalaal, M.; Ganji, D.D.; Ahmadi, G. Analytical investigation on acceleration motion of a vertically falling spherical particle in incompressible Newtonian media. *Adv. Powder Technol.* **2010**, *21*, 298–304. [CrossRef]
7. Barati, R.; Neyshabouri, S.A.A.S.; Ahmadi, G. Development of empirical models with high accuracy for estimation of drag coefficient of flow around a smooth sphere: An evolutionary approach. *Powder Technol.* **2014**, *257*, 11–19. [CrossRef]
8. Nouri, R.; Ganji, D.; Hatami, M. Unsteady sedimentation analysis of spherical particles in Newtonian fluid media using analytical methods. *Propuls. Power Res.* **2014**, *3*, 96–105. [CrossRef]
9. Yang, H.; Fan, M.; Liu, A.; Dong, L. General formulas for drag coefficient and settling velocity of sphere based on theoretical law. *Int. J. Min. Sci. Technol.* **2015**, *25*, 219–223. [CrossRef]
10. Rooki, R.; Doulati Ardejani, F.; Moradzadeh, A.; Kelessidis, V.C.; Nourozi, M. Prediction of terminal velocity of solid spheres falling through Newtonian and non-Newtonian pseudoplastic power law fluid using artificial neural network. *Int. J. Miner. Process.* **2012**, *110*, 53–61. [CrossRef]
11. Hazzab, A.; Terfous, A.; Ghenaim, A. Measurement and modeling of the settling velocity of isometric particles. *Powder Technol.* **2008**, *184*, 105–113. [CrossRef]
12. Kheloufi, N.; Lounis, M. Viscosity measurement using optical tracking of free fall in Newtonian fluid. *Acta Phys. Pol.* **2015**, *128*, 123–127. [CrossRef]
13. Sulaymon, A.H.; Wilson, C.A.M.E.; Alwared, A.I. An experimental investigation of the settling behavior of two spheres in a power law fluid. *J. Non-Newton. Fluid Mech.* **2013**, *192*, 29–36. [CrossRef]
14. Dash, S.M.; Lee, T.S. Two spheres sedimentation dynamics in a viscous liquid column. *Comput. Fluids* **2015**, *123*, 218–234. [CrossRef]
15. Luo, K.; Wei, A.; Wang, Z.; Fan, J. Fully-resolved DNS study of rotation behaviors of one and two particles settling near a vertical wall. *Powder Technol.* **2013**, *245*, 115–125. [CrossRef]
16. Tsai, L.-H.; Chang, C.-C.; Pan, T.-W.; Glowinski, R. Numerical study of the wall effect on particle sedimentation. *Int. J. Comput. Fluid Dyn.* **2018**, *32*, 158–166. [CrossRef]
17. Fidleris, V.; Whitmore, R. Experimental determination of the wall effect for spheres falling axially in cylindrical vessels. *Br. J. Appl.* **1961**, *12*, 490. [CrossRef]
18. Feng, Z.-G.; Michaelides, E.E. Inclusion of heat transfer computations for particle laden flows. *Phys. Fluids* **2008**, *20*, 040604. [CrossRef]
19. Ström, H.; Sasic, S. A multiphase DNS approach for handling solid particles motion with heat transfer. *Int. J. Multiph. Flow* **2013**, *53*, 75–87. [CrossRef]
20. Hashemi, Z.; Abouali, O.; Kamali, R. Three dimensional thermal Lattice Boltzmann simulation of heating/cooling spheres falling in a Newtonian liquid. *Int. J. Therm. Sci.* **2014**, *82*, 23–33. [CrossRef]
21. Majlesara, M.; Abouali, O.; Kamali, R.; Ardekani, M.N.; Brandt, L. Numerical study of hot and cold spheroidal particles in a viscous fluid. *Int. J. Heat Mass Transf.* **2020**, *149*, 119206. [CrossRef]
22. Li, J.-C.; Wei, Y.-J.; Wang, C.; Xia, W.-X. Drag reduction characteristics of heated spheres falling into water. *Chin. Phys. B* **2018**, *27*, 124703. [CrossRef]
23. Jetly, A.; Vakarelski, I.U.; Yang, Z.; Thoroddsen, S.T. Giant drag reduction on Leidenfrost spheres evaluated from extended free-fall trajectories. *Exp. Therm. Fluid Sci.* **2019**, *102*, 181–188. [CrossRef]
24. Mehri, A.; Akbarzadeh, P. Hydrodynamic characteristics of heated/non-heated and grooved/un-grooved spheres during free-surface water entry. *J. Fluids Struct.* **2020**, *97*, 103100. [CrossRef]
25. Wang, X.; Lyu, X. Experimental study on vertical water entry of twin spheres side-by-side. *Ocean. Eng.* **2021**, *221*, 108508. [CrossRef]
26. Beckwith, T.G.; Buck, N.L.; Marangoni, R.D. *Mechanical Measurements*; Addison-Wesley Reading: Boston, MA, USA, 1969; Volume 5.
27. Ferreira, J.M.; Duarte Naia, M.; Chhabra, R.P. An Analytical Study Of The Transient Motion Of A Dense Rigid Sphere In An Incompressible Newtonian Fluid. *Chem. Eng. Commun.* **1998**, *168*, 45–58. [CrossRef]